Series expansion method for determination of order of 3-dimensional bar-joint mechanism with arbitrarily inclined hinges

Watada, Ryo; Ohsaki, Makoto

Series expansion method for determination of order of 3-dimensional bar-joint mechanism with arbitrarily inclined hinges

Ryo WATADA[a,b], Makoto OHSAKI[a]

[a] *Department of Architecture and Architectural Engineering, Kyoto University, Kyoto-Daigaku Katsura, Nishikyo, Kyoto 615-8540, Japan*
[b] *Takenaka Corporation, 4-1-13, Hommachi, Chuo, Osaka 541-0053, Japan*

Abstract

A general method for evaluating the order of infinitesimal mechanism is presented for 3-dimensional bar-joint mechanism, which is defined as assembly of rigid bars connected to nodes by hinges with arbitrarily inclined directions. Compatibility conditions of translations and rotations are derived at bar-ends with respect to the generalized displacements consisting of displacements and rotations of nodes and bars. Degree of kinematic indeterminacy is computed using singular value decomposition of the linearized compatibility matrix. The order of infinitesimal mechanism is determined by the existence condition of higher-order coefficients of the generalized displacements with respect to the path parameter of deformation. The coefficients are obtained in a similar manner as stability analysis of geometrically nonlinear structures, where symbolic computation software package is used for analytical derivation of equations. The detailed procedure of analysis is shown through the numerical examples of a two-bar and a four-bar linkages, and the results are verified using a finite element analysis software.

Keywords: bar-joint mechanism, arbitrarily inclined hinge, singular value decomposition, series expansion, order of mechanism

Email addresses: se.watada@archi.kyoto-u.ac.jp (Ryo WATADA), ohsaki@archi.kyoto-u.ac.jp (Makoto OHSAKI)

1. Introduction

A linkage mechanism that can have infinitesimal deformation without external load is called infinitesimal mechanism. By contrast, a mechanism is called finite mechanism if it can have large deformation without external load. We consider bar-joint mechanism consisting of rigid bars connected by revolute joints, or hinges for brevity, in arbitrary directions.

A bar-joint mechanism has order [1, 2, 3]. Tarnai [1] defined the order of pin-jointed bar mechanism as: *An infinitesimal mechanism is of order* n $(n \geq 1)$ *if there exists a system of infinitesimal displacements of joints such that the coefficients of series expansion of elongation vanishes up to order* n *in all bars, but the* $(n+1)$*th coefficient does not vanish in at least one member.* Generalized Maxwell's rule and the method using singular value decomposition (SVD) [4] have been presented for evaluating the property of mechanism; however, they cannot distinguish first order and higher order mechanisms. Most of the previous studies considering the order of mechanisms focus on planar bar-joint systems. Chen [5] defined local mobility and global mobility, where first-order local mobility is equivalent to the condition for first-order mechanism, and global mobility corresponds to finite mechanism. He proposed an approach to find the order of local mobility in a general form; however, specific compatibility conditions for simple linkages are used.

Stability of bar-joint systems is also studied in the field of prestressed structures [6, 7], structural rigidity [8], and combinatorial rigidity [9]. If we regard the unstable linkage mechanism as a structure at a singular point of equilibrium state, we can use various general methods of stability analysis. For the estimation of high-order instability of structure near the singular point of equilibrium under static loads, Koiter's asymptotic expansion method can be applied [10, 11, 12]. The expansion method can also be used when singular points are multiple [13]. Salerno [2] determined the order of planar bar-joint mechanisms by the condition that the coefficients of series expansion of strains of the bars with respect to the path parameter of deformation become zero, and showed that the method can also be applied when the number of unstable modes, which is also called degree of freedom of mechanism, is greater than one. Garcea et al. [14] used Green's strain measure to truncate the higher-order terms.

There exist some analytical approaches to evaluation of the order of 3-dimensional mechanisms of bars connected by hinges, for example, Bricard

linkages, Goldberg linkages, etc. [15]. Chen et al. [16] showed the existence of the bifurcation point on the deformation path of a 6R Bricard linkage. However, they used explicit compatibility conditions of the specific linkage mechanism, and no general procedure was developed. A general linkage mechanism with links and hinges in arbitrary directions in 3-dimensional space can be modeled as bars connected by inclined revolute joints [17, 18]. However, they considered only infinitesimal deformation when obtaining mechanism solving an optimization problem that is regarded as a limit analysis problem based on the lower bound theorem.

It is not straightforward to extend the standard series expansion, which has been used in Refs. [2, 3] to generate bar-joint mechanism of a structure with ideal pin-jointed bars (truss structure), to general 3-dimensional mechanism. Since large rotation is not a vector value, many studies have been done on large deformation analysis of frames, e.g., [19, 20, 21]. Therefore, to propose an expansion method for the mechanisms of 3-dimensional bar-joint frames with hinges, we must consider an approach to express the large rotation and compatibility condition of revolute joint.

In this paper, we present a general method for evaluating the order of general 3-dimensional bar-joint mechanism, which is defined as assemblies of rigid bars connected to nodes by hinges in arbitrary directions. In Sec.2, nonlinear compatibility conditions of translations and rotations are derived at bar-ends with respect to the generalized displacements including displacements and rotations of nodes and bars. We propose the definition of the bar-ends using the translation and rotation at the center of bar, which is effective because we consider only rigid displacement and rotation of bars rather than considering deformation of bars in [19, 20, 21]. In Secs. 3 and 4, the compatibility conditions are expanded with respect to the path parameter of deformation, and the order of mechanism, as mentioned above in reference to [1], is determined by the existence condition of higher-order coefficients. Note that the terms infinitesimally rigid and infinitesimally flex are used in the field of structural rigidity; however, in this paper, we use the terminologies in structural mechanics. The detailed procedure of the analysis is shown through the numerical examples of a two-bar and a four-bar linkages [22].

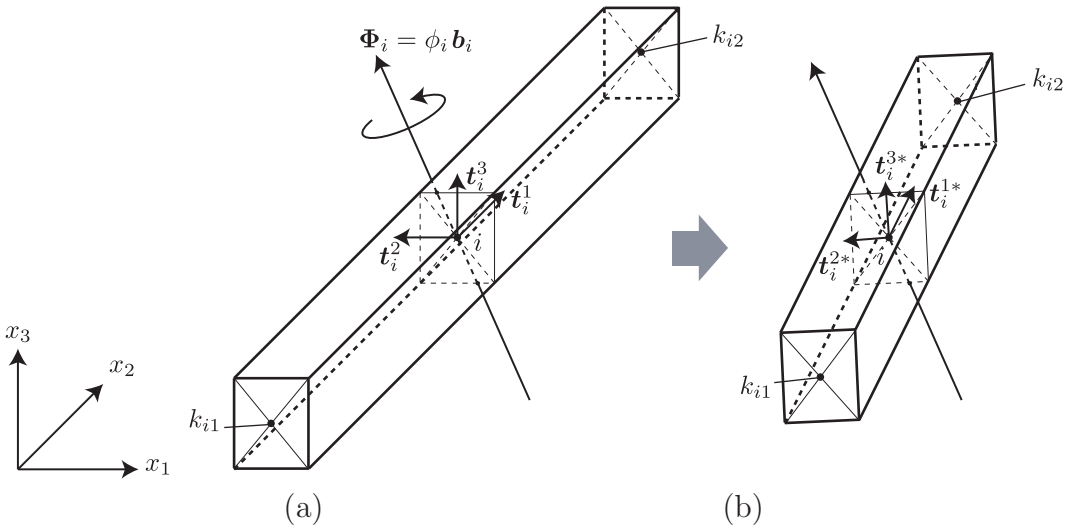

Figure 1: Definition of global coordinates, unit vectors in local coordinates, and bar rotation; (a) before deformation, (b) after deformation.

2. Compatibility equations of bar-joint mechanism with arbitrarily inclined hinges

2.1. Translation and rotation of nodes and bars

We consider a bar-joint mechanism with arbitrarily inclined hinges. Let K and M denote the set of indices of nodes (joints) and bars. Note that it is not necessary to have hinges at all bar-ends; i.e., some bars are rigidly connected to nodes.

The initial coordinates of node $k \in K$ in undeformed state and the length of bar $i \in M$ are denoted by $\boldsymbol{X}_k \in \mathbb{R}^3$ and L_i, respectively. Nodes at two ends of the ith bar are denoted as $k_{i1}, k_{i2} \in K$. We define the reference frame of undeformed state using the unit vector $\boldsymbol{t}_i^1$ directed from the center of bar i to node k_{i2} and unit vectors $\boldsymbol{t}_i^2$ and $\boldsymbol{t}_i^3$ satisfying $\boldsymbol{t}_i^1 \times \boldsymbol{t}_i^2 = \boldsymbol{t}_i^3$ and $\boldsymbol{t}_i^2 \times \boldsymbol{t}_i^3 = \boldsymbol{t}_i^1$ as shown in Fig. 1(a). The vectors directing from the center of bar i to both ends connected to nodes k_{i1} and k_{i2} are denoted by $\boldsymbol{r}_{i1}$ and $\boldsymbol{r}_{i2}$, respectively; i.e.,

$$\boldsymbol{r}_{i1} = -\frac{L_i}{2}\boldsymbol{t}_i^1, \quad \boldsymbol{r}_{i2} = \frac{L_i}{2}\boldsymbol{t}_i^1 \tag{1}$$

Note that the vectors $\boldsymbol{r}_{i1}$ and $\boldsymbol{r}_{i2}$ have the same length $L_i/2$.

Deformation of bar-joint mechanism is defined by translation and rotation of nodes and bars. The translation vector of node k in the direction of global coordinates (x_1, x_2, x_3) is denoted by $\boldsymbol{U}_k = (U_k^1, U_k^2, U_k^3)^\top \in \mathbb{R}^3$. The rotation vector of node k around global axes is denoted by $\boldsymbol{\Theta}_k = (\Theta_k^1, \Theta_k^2, \Theta_k^3)^\top \in \mathbb{R}^3$. The translation vector $\boldsymbol{V}_i = (V_i^1, V_i^2, V_i^3)^\top \in \mathbb{R}^3$ of the center of bar i is defined similarly.

The rotation vector $\boldsymbol{\Phi}_i = (\Phi_i^1, \Phi_i^2, \Phi_i^3)^\top$ at the center of bar i is defined by the unit vector $\boldsymbol{b}_i$ of the axis of rotation and the angle ϕ_i as

$$\boldsymbol{\Phi}_i = \phi_i \boldsymbol{b}_i \tag{2}$$

We define the reference frame $\boldsymbol{t}_i^{l*}$ $(l = 1, 2, 3)$ in deformed state, as shown in Fig. 1(b), by rotating $\boldsymbol{t}_i^l$ $(l = 1, 2, 3)$ around the axis $\boldsymbol{b}_i$ by the angle ϕ_i as follows [23, 24]:

$$\boldsymbol{t}_i^{l*} = \boldsymbol{b}_i(\boldsymbol{b}_i \cdot \boldsymbol{t}_i^l) + [\boldsymbol{t}_i^l - \boldsymbol{b}_i(\boldsymbol{b}_i \cdot \boldsymbol{t}_i^l)] \cos\phi_i - (\boldsymbol{t}_i^l \times \boldsymbol{b}_i) \sin\phi_i \tag{3}$$

The vectors $\boldsymbol{r}_{i1}^*$ and $\boldsymbol{r}_{i2}^*$ are defined similarly by rotating $\boldsymbol{r}_{i1}$ and $\boldsymbol{r}_{i2}$, respectively, along the axis $\boldsymbol{b}_i$ by the angle ϕ_i.

Note that a different formulation for large rotation is possible, e.g., using Euler parameters. However, it is known based on Euler's theorem of rotation of reference frame [24] that any pair of reference frames with the same origin can be transformed with each other by a single rotation along an axis. Furthermore, continuously varying configuration is investigated by carrying out series expansion from the initial undeformed state, and the parameters should be uniquely defined from the initial and final configurations. Therefore, we use the formulation in (3) involving three independent parameters.

Assuming that the center of bar i and nodes k_{i1} and k_{i2} move independently, let $\Delta\boldsymbol{U}_{i1}$ and $\Delta\boldsymbol{U}_{i2} \in \mathbb{R}^3$ denote the vectors of translational incompatibility at two ends of bar i. The vectors of rotational incompatibility at two bar-ends are denoted by $\Delta\boldsymbol{\Theta}_{i1}$ and $\Delta\boldsymbol{\Theta}_{i2} \in \mathbb{R}^3$.

If the bars are rigidly connected to nodes, the compatibility conditions are given as

$$\Delta\boldsymbol{U}_{ij} = \boldsymbol{U}_{k_{ij}} - (\boldsymbol{V}_i + \boldsymbol{r}_{ij}^*) + \boldsymbol{r}_{ij} = \boldsymbol{0} \quad (j = 1, 2,\ i \in M) \tag{4}$$

$$\Delta\boldsymbol{\Theta}_{ij} = \boldsymbol{\Theta}_{k_{ij}} - \boldsymbol{\Phi}_i = \boldsymbol{0} \quad (j = 1, 2,\ i \in M) \tag{5}$$

2.2. Inclined hinge at bar-end

We add rotational degrees of freedom at bar-ends, where arbitrarily inclined hinges are expected to exist [18]. In the example of four-bar mechanism, we add two hinges at bar ends connected to a node as shown in Fig. 2

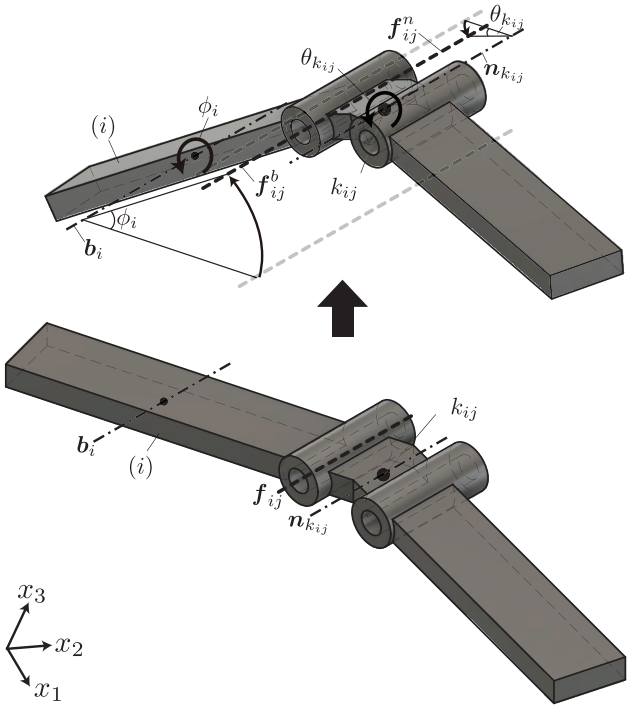

Figure 2: Illustration of hinges at bar-ends.

to clearly investigate symmetry properties of nodal displacements and self-equilibrium force modes. Since the directions of two hinges at a node are the same, the two hinges can easily be combined to obtain a model with a single hinge at each node by regarding summation of rotational angles of the two hinges as the rotation angle of the single hinge.

The rotation vector $\boldsymbol{\Theta}_k$ of node k is defined by the unit vector $\boldsymbol{n}_k$ of the axis of rotation and the angle θ_k as

$$\boldsymbol{\Theta}_k = \theta_k \boldsymbol{n}_k \tag{6}$$

Let $\boldsymbol{f}_{ij}$ denote the direction vector of the hinge between node k_{ij} and bar i. The direction vectors $\boldsymbol{f}^n_{ij}$ and $\boldsymbol{f}^b_{ij}$ after rotations of nodes and bars, respectively, are computed as

$$\boldsymbol{f}^b_{ij} = \boldsymbol{b}_i(\boldsymbol{b}_i \cdot \boldsymbol{f}_{ij}) + [\boldsymbol{f}_{ij} - \boldsymbol{b}_i(\boldsymbol{b}_i \cdot \boldsymbol{f}_{ij})]\cos\phi_i - (\boldsymbol{f}_{ij} \times \boldsymbol{b}_i)\sin\phi_i \tag{7}$$

$$\boldsymbol{f}^n_{ij} = \boldsymbol{n}_{k_{ij}}(\boldsymbol{n}_{k_{ij}} \cdot \boldsymbol{f}_{ij}) + [\boldsymbol{f}_{ij} - \boldsymbol{n}_{k_{ij}}(\boldsymbol{n}_{k_{ij}} \cdot \boldsymbol{f}_{ij})]\cos\theta_{k_{ij}} - (\boldsymbol{f}_{ij} \times \boldsymbol{n}_{k_{ij}})\sin\theta_{k_{ij}} \tag{8}$$

The compatibility conditions are given as the collinearity of vectors $\boldsymbol{f}_{ij}^{n}$ and $\boldsymbol{f}_{ij}^{b}$, which is expressed using the vector product as [24, 25]

$$\boldsymbol{e}_{ij} = \boldsymbol{f}_{ij}^{b} \times \boldsymbol{f}_{ij}^{n} = \boldsymbol{0} \tag{9}$$

Note that (9) defines three equations; however, the independent two components of (9) should be used. Such components are formally written as

$$\boldsymbol{e}_{ij}^{(2)} = (e_{ij}^{1}, e_{ij}^{2})^{\top} = \boldsymbol{0} \tag{10}$$

The condition (5) is to be replaced by (10) if a hinge exists at the jth end of bar i, which means that number of constraints is reduced by one, when a hinge is placed at a bar end.

The compatibility conditions are combined into $\boldsymbol{G} = \boldsymbol{0}$. Accordingly, the vector $\boldsymbol{G}$ is called *incompatibility vector*. Similarly, the *generalized displacement vector* $\boldsymbol{W}$ is defined as an assemblage of $\boldsymbol{U}$, $\boldsymbol{\Theta}$, $\boldsymbol{V}$, and $\boldsymbol{\Phi}$. Note that ϕ_i and $\boldsymbol{b}_i$ are functions of $\boldsymbol{\Phi}$, and θ_k and $\boldsymbol{n}_k$ are functions of $\boldsymbol{\Theta}$.

Let m_0, n_0, and s denote the numbers of bars, nodes, and constrained degrees of freedom, respectively. When we have h hinges, the numbers of components of $\boldsymbol{W}$ and $\boldsymbol{G}$, denoted by n and m, respectively, are determined as $n = 6n_0 + 6m_0 - s$ and $m = 12m_0 - h$.

3. Derivation of first-order infinitesimal mechanism and self-equilibrium forces

3.1. Condition of first-order infinitesimal mechanism

In this and next sections, we show a general method to analyze "incompatibiliy function" using series expansion for any kind of mechanisms including the specific mechanism defined in the previous section.

Deformed configuration of a bar-joint mechanism is defined in terms of the generalized displacement vector $\boldsymbol{W}$. Following the standard procedure of geometrically nonlinear analysis, the vector $\boldsymbol{W}$ is parameterized in terms of a path parameter ξ [12].

In the following, we use $(\,)'$ to indicate the derivative with respect to ξ, and adopt summation convention when an index is repeated in one term.

The incompatibility vector $\boldsymbol{G}$ is a function of $\boldsymbol{W}(\xi)$ as $\boldsymbol{G}(\boldsymbol{W}(\xi))$. If the bar-joint system has a mechanism such that it deforms without external load,

there exists a non-zero $\boldsymbol{W}$ satisfying the following compatibility condition along the path of deformation:

$$\boldsymbol{G}(\boldsymbol{W}(\xi)) = \boldsymbol{0} \tag{11}$$

We omit the argument ξ for simple expression of equations. Differentiating (11) with respect to ξ, we obtain

$$\frac{\partial G_s}{\partial W_i} W_i' = 0 \quad (s = 1, \ldots, m) \tag{12}$$

Evaluating at $\xi = 0$, (12) is written simply as

$$\boldsymbol{\Gamma} \boldsymbol{W}' = \boldsymbol{0} \tag{13}$$

where $\boldsymbol{\Gamma} \in \mathbb{R}^{m \times n}$ is a constant matrix of which the (s, i) component Γ_{si} is defined as

$$\Gamma_{si} = \left. \frac{\partial G_s}{\partial W_i} \right|_{\xi=0} \tag{14}$$

In the following, all variables are evaluated at the undeformed state $\xi = 0$. If any non-zero $\boldsymbol{W}'$ satisfying (13) is found, the bar-joint system has at least first-order infinitesimal mechanism.

Since $\boldsymbol{\Gamma}$ is derived by differentiation of the compatibility conditions with respect to the generalized displacements, it may be regarded as a generalized compatibility matrix. Therefore, *generalized self-equilibrium force vector* is defined as the vector $\boldsymbol{F} \in \mathbb{R}^m$ satisfying

$$\boldsymbol{F}^\top \boldsymbol{\Gamma} = \boldsymbol{0} \tag{15}$$

which is also expressed as

$$F_s \frac{\partial G_s}{\partial W_i} = 0 \quad (i = 1, \ldots, n) \tag{16}$$

It is easily seen that the components of $\boldsymbol{F}$ corresponding to translational incompatibility in $\boldsymbol{G}$ are regarded as the bar-end forces.

3.2. Singular value decomposition of $\boldsymbol{\Gamma}$

Using SVD, $\boldsymbol{\Gamma}$ is decomposed as [26]

$$\boldsymbol{\Gamma} = \boldsymbol{B} \boldsymbol{\Sigma} \boldsymbol{H}^\top \tag{17}$$

Defining $r = \mathrm{rank}(\boldsymbol{\Gamma})$, $p = n - r$, and $q = m - r$, we can express matrices $\boldsymbol{\Sigma}$, $\boldsymbol{H}$, and $\boldsymbol{B}$ as

$$\boldsymbol{\Sigma} = \begin{bmatrix} \mathrm{diag}(\lambda_1, \ldots, \lambda_r) & \boldsymbol{O}_{r\times p} \\ \boldsymbol{O}_{q\times r} & \boldsymbol{O}_{q\times p} \end{bmatrix} \in \mathbb{R}^{m\times n} \tag{18}$$

$$\boldsymbol{H} = [\boldsymbol{\eta}_1, \ldots, \boldsymbol{\eta}_n] \in \mathbb{R}^{n\times n} \tag{19}$$

$$\boldsymbol{B} = [\boldsymbol{\beta}_1, \ldots, \boldsymbol{\beta}_m] \in \mathbb{R}^{m\times m} \tag{20}$$

where the singular values are ordered as $\lambda_1 \geq \cdots \geq \lambda_r$, and $\boldsymbol{H}$ and $\boldsymbol{B}$ are orthogonal matrices consisting of singular vectors.

Post-multiplying $\boldsymbol{H}$ to both sides of (17), we obtain

$$\boldsymbol{\Gamma}\boldsymbol{\eta}_j = \begin{cases} \lambda_j \boldsymbol{\beta}_j & (j = 1, \ldots, r) \\ \boldsymbol{0} & (j = r+1, \ldots, n) \end{cases} \tag{21}$$

Furthermore, pre-multiplying $\boldsymbol{B}^\top$ to both sides of (17), we have

$$\boldsymbol{\beta}_i^\top \boldsymbol{\Gamma} = \begin{cases} \lambda_i \boldsymbol{\eta}_i^\top & (i = 1, \ldots, r) \\ \boldsymbol{0}^\top & (i = r+1, \ldots, m) \end{cases} \tag{22}$$

Let $\mathrm{im}(\boldsymbol{\Gamma})$ and $\ker(\boldsymbol{\Gamma})$ be the column space and the null space [26] of $\boldsymbol{\Gamma}$. Then (21) shows that $\boldsymbol{\beta}_1, \ldots, \boldsymbol{\beta}_r$ are the bases of $\mathrm{im}(\boldsymbol{\Gamma})$, and $\boldsymbol{\eta}_{r+1}, \ldots, \boldsymbol{\eta}_{r+p}$ are the bases of $\ker(\boldsymbol{\Gamma})$. Similarly, we can find from (22) that $\boldsymbol{\eta}_1, \ldots, \boldsymbol{\eta}_r$ are the bases of the row space $\mathrm{im}(\boldsymbol{\Gamma})$, and $\boldsymbol{\beta}_{r+1}, \ldots, \boldsymbol{\beta}_{r+q}$ are the bases of the left null space $\ker(\boldsymbol{\Gamma}^\top)$.

Eq. (13) shows that an first-order infinitesimal mechanism $\boldsymbol{W}'$ is expressed as a linear combination of the bases of $\ker(\boldsymbol{\Gamma})$. Therefore, the vectors $\boldsymbol{\eta}_{r+1}, \ldots, \boldsymbol{\eta}_{r+p}$ represent the first-order infinitesimal mechanism modes, and p is the number of mechanisms, which is equal to the number of kinematic indeterminacy.

Similarly, (15) shows that the generalized self-equilibrium force vector $\boldsymbol{F}$ is written as a linear combination of the bases $\boldsymbol{\beta}_{r+1}, \ldots, \boldsymbol{\beta}_{r+p}$ of $\ker(\boldsymbol{\Gamma}^\top)$, where q is the number of self-equilibrium modes, which is equal to the number of statical indeterminacy.

For simplicity, hereinafter we reverse the order of singular values and vectors; i.e., we rename $\boldsymbol{\eta}_n, \ldots, \boldsymbol{\eta}_1$ as $\boldsymbol{\eta}_1, \ldots, \boldsymbol{\eta}_n$, $\boldsymbol{\beta}_m, \ldots, \boldsymbol{\beta}_1$ as $\boldsymbol{\beta}_1, \ldots, \boldsymbol{\beta}_m$ and $\lambda_1, \ldots, \lambda_r$ as $\lambda_r, \ldots, \lambda_1$, respectively.

4. Conditions of higher-order infinitesimal mechanisms

Assuming that a frame has a single first-order infinitesimal mechanism mode, i.e., $p = 1$ and $\boldsymbol{W}' = \boldsymbol{\eta}_1$, we investigate the existence of higher order terms of the mechanism.

The generalized displacement vector $\boldsymbol{W}(\xi)$ is expressed as a linear combination of the right singular vectors as

$$\boldsymbol{W} = \xi\boldsymbol{\eta}_1 + \alpha_2\boldsymbol{\eta}_2 + \cdots + \alpha_n\boldsymbol{\eta}_n \tag{23}$$

where $\boldsymbol{\eta}_1$ is a first-order infinitesimal mechanism mode and $\alpha_j(\xi)$ $(j = 2, \ldots, n)$ are the coefficients of the basis vectors for the row space of $\mathrm{im}(\boldsymbol{\Gamma})$. Note that $\alpha_j(\xi)$ is a function of the path parameter ξ.

Pre-multiplying $\boldsymbol{\eta}_1^\top$ to the both sides of (23), we have

$$\boldsymbol{\eta}_1^\top \boldsymbol{W} = \xi \tag{24}$$

Differentiating the both sides of (24) successively with respect to ξ, we obtain

$$\boldsymbol{\eta}_1^\top \boldsymbol{W}' = 1 \tag{25}$$

$$\boldsymbol{\eta}_1^\top \boldsymbol{W}'' = \boldsymbol{\eta}_1^\top \boldsymbol{W}''' = \cdots = 0 \tag{26}$$

Assuming the first-order infinitesimal mechanism $\boldsymbol{W}'$ is obtained, we investigate the condition for existence of second order mechanism. Differentiation of (12) with respect to ξ leads to

$$\frac{\partial^2 G_s}{\partial W_i \partial W_j} W_i' W_j' + \frac{\partial G_s}{\partial W_i} W_i'' = 0 \quad (s = 1, \ldots, m) \tag{27}$$

From (27), $\boldsymbol{W}''$ is determined as the solution of the following set of linear equations:

$$\boldsymbol{\Gamma}\boldsymbol{W}'' = \boldsymbol{g}^{(2)} \tag{28}$$

where $\boldsymbol{g}^{(2)} \in \mathbb{R}^m$ is a constant vector calculated from $\boldsymbol{W}'$ as

$$g_s^{(2)} = -\left.\frac{\partial^2 G_s}{\partial W_i \partial W_j}\right|_{\xi=0} W_i' W_j' \quad (s = 1, \ldots, m) \tag{29}$$

If there exists $\boldsymbol{W}''$ satisfying (28), the bar-joint mechanism is at least second order. Note that (28) has the solution $\boldsymbol{W}''$ if and only if $\boldsymbol{g}^{(2)} \in \mathrm{im}(\boldsymbol{\Gamma})$; i.e., $\boldsymbol{g}^{(2)}$ is orthogonal to all basis vectors of $\ker(\boldsymbol{\Gamma}^\top)$. Conditions for existence of $\boldsymbol{W}''$ for the cases $q = 0$ and $q \geq 1$, respectively, are summarized as follows:

(a) $q = 0$
In this case, $\ker(\boldsymbol{\Gamma}^\top)$ has no basis and (28) always has a solution.

(b) $q \geq 1$
The bases of $\ker(\boldsymbol{\Gamma}^\top)$ are self-equilibrium force modes $\boldsymbol{\beta}_1, \ldots, \boldsymbol{\beta}_q$; thus $\boldsymbol{W}''$ exists when the following equations hold:

$$\boldsymbol{\beta}_i^\top \boldsymbol{g}^{(2)} = 0 \quad (i = 1, \ldots, q) \tag{30}$$

Note that we can regard $\boldsymbol{g}^{(2)}$ as a second-order generalized strain vector generated by $\boldsymbol{W}'$. Therefore, (30) indicates that the works done by the forces $\boldsymbol{\beta}_1, \ldots, \boldsymbol{\beta}_q$ against the strain $\boldsymbol{g}^{(2)}$ vanish.

When one of the conditions (a) and (b) is satisfied, we can obtain $\boldsymbol{W}''$ by pre-multiplying $\boldsymbol{\beta}_i^\top$ $(i = q+1, \ldots, m)$ to both sides of (28) as

$$\boldsymbol{W}'' = \alpha''_{p+1}\boldsymbol{\eta}_{p+1} + \cdots + \alpha''_n \boldsymbol{\eta}_n \tag{31}$$

$$\alpha''_{p+i} = \frac{\boldsymbol{\beta}_{q+i}^\top \boldsymbol{g}^{(2)}}{\lambda_i} \quad (i = 1, \ldots, r) \tag{32}$$

Therefore, each of (a) and (b) is a sufficient condition for existence of second order infinitesimal mechanism.

We can investigate the condition for existence of third order infinitesimal mechanism in the same manner. Differentiating (27) with respect to ξ, we have

$$\frac{\partial^3 G_s}{\partial W_i \partial W_j \partial W_k} W_i' W_j' W_k' + 3\frac{\partial^2 G_s}{\partial W_i \partial W_j} W_i'' W_j' + \frac{\partial G_s}{\partial W_i} W_i''' = 0 \quad (s = 1, \ldots, m) \tag{33}$$

From (33), we obtain a set of equations for $\boldsymbol{W}'''$ as

$$\boldsymbol{\Gamma} \boldsymbol{W}''' = \boldsymbol{g}^{(3)} \tag{34}$$

where $\boldsymbol{g}^{(3)} \in \mathbb{R}^m$ is a constant vector calculated from $\boldsymbol{W}'$ and $\boldsymbol{W}''$ as

$$g_s^{(3)} = -\left.\frac{\partial^3 G_s}{\partial W_i \partial W_j \partial W_k}\right|_{\xi=0} W_i' W_j' W_k' - 3\left.\frac{\partial^2 G_s}{\partial W_i \partial W_j}\right|_{\xi=0} W_i'' W_j' \quad (s = 1, \ldots, m) \tag{35}$$

The conditions for existence of $\boldsymbol{W}'''$ is same as that of $\boldsymbol{W}''$, where (30) for (b) is replaced with

$$\boldsymbol{\beta}_i^\top \boldsymbol{g}^{(3)} = 0 \quad (i = 1, \ldots, q) \tag{36}$$

When $\boldsymbol{W}'''$ exists, we can calculate it as

$$\boldsymbol{W}''' = \alpha'''_{p+1}\boldsymbol{\eta}_{p+1} + \cdots + \alpha'''_{n}\boldsymbol{\eta}_{n} \tag{37}$$

$$\alpha'''_{p+i} = \frac{\boldsymbol{\beta}_{q+i}^{\top}\boldsymbol{g}^{(3)}}{\lambda_i} \ (i = 1, \ldots, r) \tag{38}$$

The conditions for existence of forth and higher order infinitesimal mechanisms can be derived in the same manner.

Finally, the deformation including higher order terms can be expressed in a series expansion form as

$$\boldsymbol{W} = \boldsymbol{W}'\xi + \frac{1}{2!}\boldsymbol{W}''\xi^2 + \frac{1}{3!}\boldsymbol{W}'''\xi^3 + \cdots \tag{39}$$

We can successively determine the terms up to arbitrary orders in (39), if the mechanism evaluated above is a finite mechanism.

Although derivation of $\dfrac{\partial G_s}{\partial W_i}$, $\dfrac{\partial^2 G_s}{\partial W_i \partial W_j}$, and $\dfrac{\partial^3 G_s}{\partial W_i \partial W_j \partial W_k}$ involves very complicated differentiation, it can be done systematically using a symbolic computation software package. Furthermore, if a general form is derived for a beam element with hinges and springs at bar ends, then it can be assembled to a frame with many bars. In the following examples, a symbolic computation software package Maple [27] Ver. 16 is used for analytical derivations of equations.

5. Numerical examples

5.1. Example 1: two-bar linkages

Orders of infinitesimal mechanism are evaluated for two models 1A and 1B as shown in Fig. 3. In both models, two bars with the same length are connected at node 2, which is indicated by a filled square. All translational and rotational components except rotation around Y-axis are constrained at node 1, and all translational components except X-directional displacement are constrained at node 3. Furthermore, each model has a hinge at the end of bar 2 connected to node 2, as indicated with dashed line in Fig. 3. The difference in two models is the direction of the hinge; the axis of the hinge of model 1A is parallel to Y-axis, while the axis of the hinge of model 1B is inclined 45 degrees from X-axis and Y-axis in XY-plane.

In both models, $m_0 = 2$, $n_0 = 3$, $h = 1$, $s = 7$, $m = 23$, and $n = 23$. SVD of $\boldsymbol{\Gamma}$ is carried out to find that $r = \mathrm{rank}(\boldsymbol{\Gamma}) = 22$ for both models. Thus, they

Table 1: Vectors $\boldsymbol{W}'$, $\boldsymbol{W}''$, and $\boldsymbol{W}'''$ of the two-bar linkages.

	model 1A			model 1B		
	$\boldsymbol{W}'$ $(=\boldsymbol{\eta}_1)$	$\boldsymbol{W}''$	$\boldsymbol{W}'''$	$\boldsymbol{W}'$ $(=\boldsymbol{\eta}_1)$	$\boldsymbol{W}''$	$\boldsymbol{W}'''$
U_1^1	0.0000	0.0000	0.0000	0.0000	0.0000	-
U_1^2	0.0000	0.0000	0.0000	0.0000	0.0000	-
U_1^3	0.0000	0.0000	0.0000	0.0000	0.0000	-
Θ_1^1	0.0000	0.0000	0.0000	0.0000	0.0000	-
Θ_1^2	0.3922	0.0000	0.0139	0.2626	0.0000	-
Θ_1^3	0.0000	0.0000	0.0000	0.0000	0.0000	-
U_2^1	0.0000	-0.1538	0.0000	0.0000	-0.0690	-
U_2^2	0.0000	0.0000	0.0000	0.0000	0.0000	-
U_2^3	-0.3922	0.0000	0.0464	-0.2626	0.0000	-
Θ_2^1	0.0000	0.0000	0.0000	0.0000	0.0000	-
Θ_2^2	0.3922	0.0000	0.0139	0.2626	0.0000	-
Θ_2^3	0.0000	0.0000	0.0000	0.0000	0.0000	-
U_3^1	0.0000	-0.3077	0.0000	0.0000	-0.1379	-
U_3^2	0.0000	0.0000	0.0000	0.0000	0.0000	-
U_3^3	0.0000	0.0000	0.0000	0.0000	0.0000	-
Θ_3^1	0.0000	0.0000	0.0000	-0.5252	0.0000	-
Θ_3^2	-0.3922	0.0000	-0.0139	-0.2626	0.0000	-
Θ_3^3	0.0000	0.0000	0.0000	0.0000	-0.1379	-
V_1^1	0.0000	-0.0769	0.0000	0.0000	-0.0345	-
V_1^2	0.0000	0.0000	0.0000	0.0000	0.0000	-
V_1^3	-0.1961	0.0000	0.0232	-0.1313	0.0000	-
Φ_1^1	0.0000	0.0000	0.0000	0.0000	0.0000	-
Φ_1^2	0.3922	0.0000	0.0139	0.2626	0.0000	-
Φ_1^3	0.0000	0.0000	0.0000	0.0000	0.0000	-
V_2^1	0.0000	-0.2308	0.0000	0.0000	-0.1034	-
V_2^2	0.0000	0.0000	0.0000	0.0000	0.0000	-
V_2^3	-0.1961	0.0000	0.0232	-0.1313	0.0000	-
Φ_2^1	0.0000	0.0000	0.0000	-0.5252	0.0000	-
Φ_2^2	-0.3922	0.0000	-0.0139	-0.2626	0.0000	-
Φ_2^3	0.0000	0.0000	0.0000	0.0000	-0.1379	-

Table 2: Vectors $\boldsymbol{\beta}_1$, $\boldsymbol{g}^{(2)}$ and $\boldsymbol{g}^{(3)}$ of the two-bar linkages

	model 1A			model 1B		
	$\boldsymbol{\beta}_1$	$\boldsymbol{g}^{(2)}$	$\boldsymbol{g}^{(3)}$	$\boldsymbol{\beta}_1$	$\boldsymbol{g}^{(2)}$	$\boldsymbol{g}^{(3)}$
ΔU_{11}^1	0.0000	0.0769	0.0000	0.0000	0.0345	0.0000
ΔU_{11}^2	0.0000	0.0000	0.0000	0.0000	0.0000	0.0000
ΔU_{11}^3	0.0000	0.0000	-0.0302	0.0000	0.0000	-0.0091
ΔU_{12}^1	0.0000	-0.0769	0.0000	0.0000	-0.0345	0.0000
ΔU_{12}^2	0.0000	0.0000	0.0000	0.0000	0.0000	0.0000
ΔU_{12}^3	0.0000	0.0000	0.0302	0.0000	0.0000	0.0091
ΔU_{21}^1	0.0000	0.0769	0.0000	0.0000	0.0345	0.0000
ΔU_{21}^2	0.0000	0.0000	0.0000	0.0000	-0.0690	0.0000
ΔU_{21}^3	0.0000	0.0000	0.0302	0.0000	0.0000	-0.0091
ΔU_{22}^1	0.0000	-0.0769	0.0000	0.0000	-0.0345	0.0000
ΔU_{22}^2	0.0000	0.0000	0.0000	0.0000	0.0690	0.0000
ΔU_{22}^3	0.0000	0.0000	-0.0302	0.0000	0.0000	0.0091
$\Delta\Theta_{11}^1$	0.0000	0.0000	0.0000	0.0000	0.0000	0.0000
$\Delta\Theta_{11}^2$	0.0000	0.0000	0.0000	0.0000	0.0000	0.0000
$\Delta\Theta_{11}^3$	0.0000	0.0000	0.0000	0.0000	0.0000	0.0000
$\Delta\Theta_{12}^1$	0.0000	0.0000	0.0000	0.0000	0.0000	0.0000
$\Delta\Theta_{12}^2$	0.0000	0.0000	0.0000	0.0000	0.0000	0.0000
$\Delta\Theta_{12}^3$	0.0000	0.0000	0.0000	0.0000	0.0000	0.0000
e_{21}^1	0.0000	0.0000	0.0000	0.7071	0.0000	-0.0272
e_{21}^2	-1.0000	0.0000	0.0000	0.7071	0.0000	-0.1902
$\Delta\Theta_{22}^1$	0.0000	0.0000	0.0000	0.0000	0.0000	0.0000
$\Delta\Theta_{22}^2$	0.0000	0.0000	0.0000	0.0000	0.0000	0.0000
$\Delta\Theta_{22}^3$	0.0000	0.0000	0.0000	0.0000	0.0000	0.0000

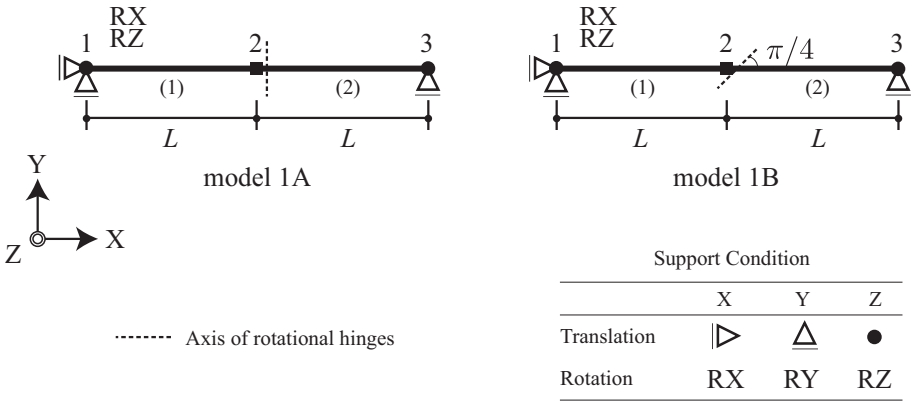

Figure 3: Models 1A and 1B of two-bar linkage.

have one first-order infinitesimal mechanism mode and one self-equilibrium force mode, because $p = q = 1$. The infinitesimal mechanism mode vector $\boldsymbol{W}'$ $(= \boldsymbol{\eta}_1)$, the self-equilibrium mode vector $\boldsymbol{\beta}_1$, and the vector $\boldsymbol{g}^{(2)}$ of both models are shown in Tables 1 and 2.

Evaluating the second order condition (30), we find that $\boldsymbol{\beta}_1^\top \boldsymbol{g}^{(2)} = 0.0000$ is satisfied for both models 1A and 1B, and the second order terms $\boldsymbol{W}''$ are calculated as shown in Table 1.

For model 1A, the third order condition $\boldsymbol{\beta}_1^\top \boldsymbol{g}^{(3)} = 0.0000$ of (36) is also satisfied by the vector $\boldsymbol{g}^{(3)}$ shown in Table 2, and we obtain $\boldsymbol{W}'''$ as shown in Table 1. However, for model 1B, $\boldsymbol{\beta}_1^\top \boldsymbol{g}^{(3)} = -0.1537$; therefore, $\boldsymbol{W}'''$ does not exist. Consequently, we can determine that the infinitesimal mechanism of model 1A is at least third order, and the infinitesimal mechanism of model 1B is second order.

5.2. Example 2: four-bar linkage

Next, we consider a square model in XY-plane as shown in Fig. 4, which has four bars connected at four nodes. This model is known as a Bennett 4R linkage [15]. Each bar has hinges at both ends, and the axes of the hinges are defined at the initial state in the global coordinate system as follows:

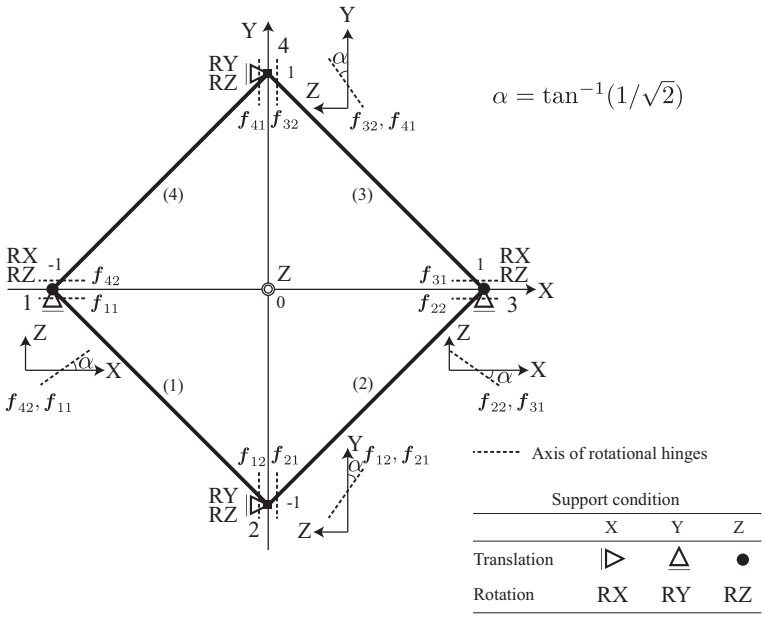

Figure 4: Four-bar linkage.

$$\boldsymbol{f}_{11} = \boldsymbol{f}_{42} = \begin{pmatrix} \sqrt{\frac{2}{3}} \\ 0 \\ \sqrt{\frac{1}{3}} \end{pmatrix}, \quad \boldsymbol{f}_{12} = \boldsymbol{f}_{21} = \begin{pmatrix} 0 \\ \sqrt{\frac{2}{3}} \\ -\sqrt{\frac{1}{3}} \end{pmatrix}$$

$$\boldsymbol{f}_{22} = \boldsymbol{f}_{31} = \begin{pmatrix} -\sqrt{\frac{2}{3}} \\ 0 \\ \sqrt{\frac{1}{3}} \end{pmatrix}, \quad \boldsymbol{f}_{32} = \boldsymbol{f}_{41} = \begin{pmatrix} 0 \\ -\sqrt{\frac{2}{3}} \\ -\sqrt{\frac{1}{3}} \end{pmatrix}$$

Although the physical model has only four hinges, the numerical model has eight hinges; i.e., there exist a pair of hinges in the same direction at a node. This way, the boundary conditions are easily assigned at nodes, and symmetry properties of deformation can be clearly observed. Note again that the rotation angles of two parallel hinges can be added to combine two hinges to one.

The support conditions are shown in Fig. 4, where $m_0 = 4$, $n_0 = 4$, $h = 8$, and $s = 14$; thus, the numbers of rows and columns of matrix $\mathbf{\Gamma}$ are

Table 3: Vectors $\boldsymbol{W}'$, $\boldsymbol{W}''$ and $\boldsymbol{W}'''$ of the four-bar linkage.

	$\boldsymbol{W}'$ $(=\boldsymbol{\eta}_1)$	$\boldsymbol{W}''$	$\boldsymbol{W}'''$
U_1^1	-0.1715	0.0294	0.0849
U_1^2	0.0000	0.0000	0.0000
U_1^3	0.0000	0.0000	0.0000
Θ_1^1	0.0000	0.0000	0.0000
Θ_1^2	-0.2425	-0.1248	-0.0441
Θ_1^3	0.0000	0.0000	0.0000
U_2^1	0.0000	0.0000	0.0000
U_2^2	0.1715	0.0294	-0.0849
U_2^3	0.0000	0.3328	0.0000
Θ_2^1	0.2425	-0.1248	0.0441
Θ_2^2	0.0000	0.0000	0.0000
Θ_2^3	0.0000	0.0000	0.0000
V_1^1	-0.0857	0.0147	0.0424
V_1^2	0.0857	0.0147	-0.0424
V_1^3	0.0000	0.1664	0.0000
Φ_1^1	0.2425	-0.1248	0.0120
Φ_1^2	-0.2425	-0.1248	-0.0120
Φ_1^3	0.1715	0.0000	0.0312

Table 4: Vectors $\boldsymbol{\beta}_j$ $(j = 1, \cdots, 7)$, $\boldsymbol{g}^{(2)}$, and $\boldsymbol{g}^{(3)}$ of bar 1 of four-bar linkage.

	$\boldsymbol{\beta}_1$	$\boldsymbol{\beta}_2$	$\boldsymbol{\beta}_3$	$\boldsymbol{\beta}_4$	$\boldsymbol{\beta}_5$	$\boldsymbol{\beta}_6$	$\boldsymbol{\beta}_7$	$\boldsymbol{g}^{(2)}$	$\boldsymbol{g}^{(3)}$
ΔU_{11}^1	-0.1313	-0.2462	-0.0191	0.0768	-0.0098	0.1245	0.1278	0.0147	0.0580
ΔU_{11}^2	-0.0879	0.0418	0.1806	-0.1825	-0.0680	-0.0029	-0.2249	-0.0147	0.0580
ΔU_{11}^3	-0.1996	0.0988	-0.0330	0.0986	0.1066	-0.1034	0.0301	-0.0416	0.0000
ΔU_{12}^1	0.1313	0.2462	0.0191	-0.0768	0.0098	-0.1245	-0.1278	-0.0147	-0.0580
ΔU_{12}^2	0.0879	-0.0418	-0.1806	0.1825	0.0680	0.0029	0.2249	0.0147	-0.0580
ΔU_{12}^3	0.1996	-0.0988	0.0330	-0.0986	-0.1066	0.1034	-0.0301	0.0416	0.0000
e_{11}^1	0.2615	0.2625	-0.0024	-0.0049	-0.2147	0.0226	0.4424	0.0416	0.0107
e_{11}^2	0.2674	-0.0418	-0.0805	-0.0222	0.0200	0.0100	-0.1089	0.0000	-0.0321
e_{12}^1	0.1124	-0.1863	0.0338	-0.0970	-0.0350	0.0959	-0.1775	0.0000	0.0321
e_{12}^2	-0.2035	-0.1712	0.3403	-0.2292	-0.3798	0.2804	0.2364	0.0416	-0.0107

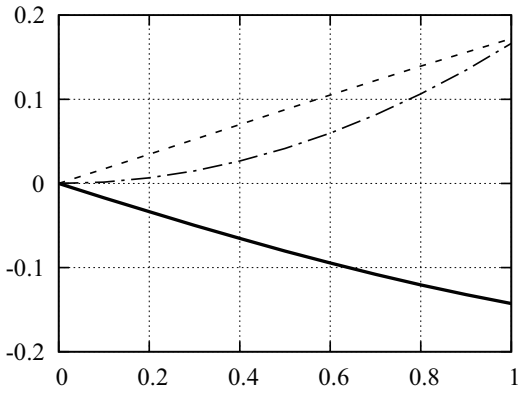

Figure 5: Nodal displacements with respect to path parameter; solid line: U_1^1, dashed line: U_2^2, chain line: U_2^3.

$m = 40$ and $n = 34$, respectively. From the SVD of $\boldsymbol{\Gamma}$, we obtain $r = 33$, and consequently, $p = n - r = 1$ and $q = m - r = 7$ are determined. Therefore, the model has one first-order infinitesimal mechanism mode $\boldsymbol{W}'$ $(= \boldsymbol{\eta}_1)$ and seven self-equilibrium force modes $\boldsymbol{\beta}_j$ $(j = 1, \cdots, 7)$. The components of $\boldsymbol{W}'$ corresponding to nodes 1, 2 and bar 1 are shown in Table 3, and the components of $\boldsymbol{\beta}_j$ $(j = 1, \cdots, 7)$ and $\boldsymbol{g}^{(2)}$ corresponding to bar 1 are shown in Table 4. We confirmed all of the seven equations $\boldsymbol{\beta}_j^\top \boldsymbol{g}^{(2)} = 0$ $(j = 1, \ldots, 7)$

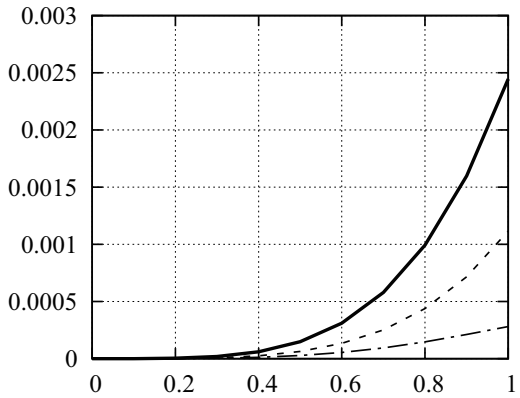

Figure 6: Errors in compatibility conditions with respect to path parameter; solid line: ΔU^1_{11}, dashed line: ΔU^3_{12}, chain line: e^1_{11}.

of the second order condition (30) are satisfied to obtain non-zero solution of $\boldsymbol{W}''$. We can find that the equations of the third order condition $\boldsymbol{\beta}_j^\top \boldsymbol{g}^{(3)} = 0$ $(j = 1, \cdots, 7)$ are also satisfied, and we can obtain $\boldsymbol{W}'''$ in the same manner.

The nodal displacements are plotted with respect to the path parameter in Fig. 5, where solid, dashed, and chain lines are U^1_1, U^2_2, and U^3_2, respectively. The errors in compatibility conditions are plotted with respect to the path parameter in Fig. 6, where solid, dashed, and chain lines are ΔU^1_1, ΔU^3_2, and e^1_1, respectively. As seen from Fig. 6, the errors in compatibility conditions are sufficiently small.

The same four-bar mechanism is analyzed using Abaqus Ver. 6.14 [28]. Forced deformation in positive and negative y-direction are applied at nodes 2 and 4, respectively. The shape at $U^2_2 = 0$, 0.08, 0.16, and 0.24 are shown in Figs. 7(a)-(d), where the short cylinders show the hinges. It is confirmed that all sectional forces and reactions vanish during deformation.

The variations of U^1_1 U^3_2 are plotted with respect to U^2_2 in Figs. 8 and 9, respectively, where solid and dashed lines are the results of series expansion and Abaqus, respectively. It is seen from the figures that the series expansion has good accuracy when the deformation is not very large.

6. Conclusion

We have presented a general method for determining the order of deformation of bar-joint mechanisms with arbitrarily inclined hinges. The conclusions

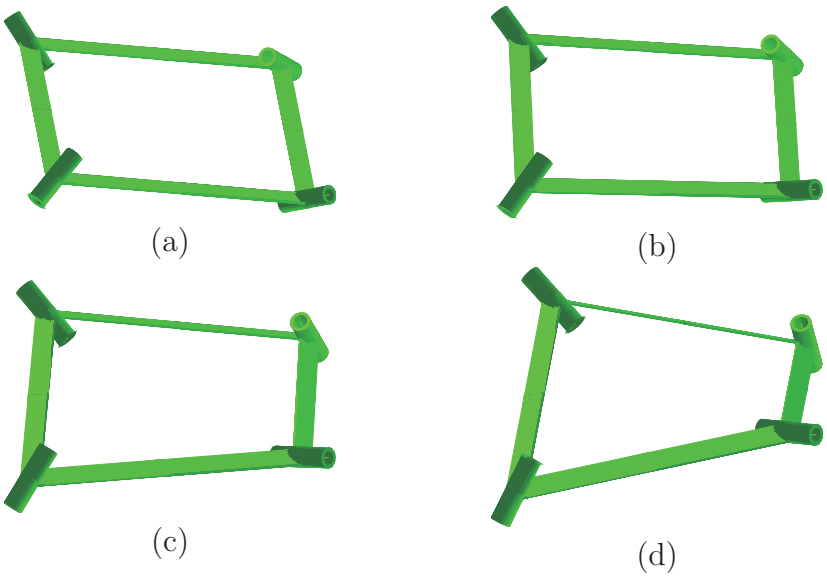

Figure 7: Results of large deformation analysis at $U_2^2 = 0$, 0.08, 0.16, and 0.24 computed using Abaqus.

drawn from this study are summarized as follows:

1. The conditions for existence of higher order terms of the infinitesimal mechanisms have been derived by successively differentiating the compatibility conditions of displacements and rotations of nodes and bars

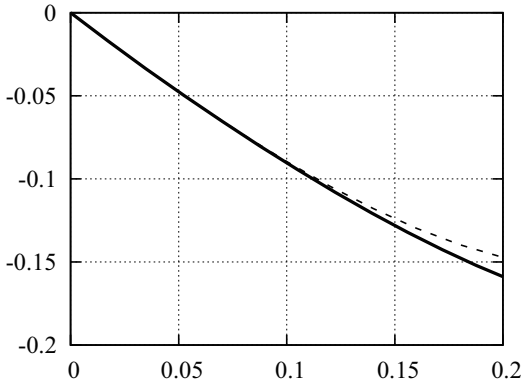

Figure 8: Variation of U_1^1 with respect to U_2^2; solid line: series expansion, dashed line: large deformation analysis.

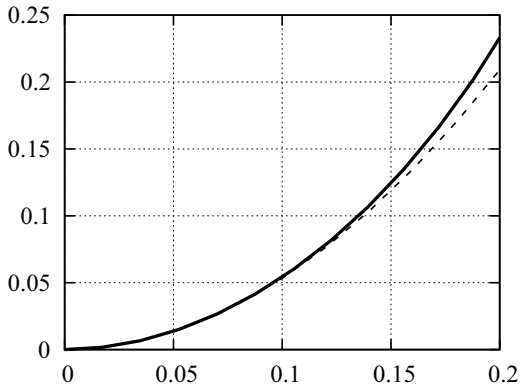

Figure 9: Variation of U_2^3 with respect to U_2^2; solid line: series expansion, dashed line: large deformation analysis.

with respect to the path parameter of deformation. Compatibility conditions at hinge are derived as the collinearity of the direction vectors of hinges after undergoing rotation of the node and bar connected to the hinge.

2. Generalized self-equilibrium force has been defined as the left singular vector corresponding to a zero singular value. It is seen from the derived conditions that the infinitesimal mechanism has higher-order terms if the higher-order generalized strain vector is orthogonal to all generalized self-equilibrium force vectors.
3. The complex formulas for higher-order terms can be systematically derived using a symbolic computation software package. If formulas are derived for a bar element with hinges at bar-ends, then the order of mechanism with several bars can be evaluated systematically.
4. Accuracy of the proposed method has been confirmed by comparing the large deformation of a four-bar mechanism computed using a finite element analysis software. It has also been shown that error in compatibility vector computed using third order expansion is negligibly small when the deformation is not very large.

Acknowledgments

This study is partly supported by JSPS Kakenhi Grant No. 26420557.

References

[1] T. Tarnai, Higher-order infinitesimal mechanisms, Acad. Sci. Hung., 102(3–4), pp. 363–378, 1989.

[2] G. Salerno, How to recognize the order of infinitesimal mechanism: A numerical approach, Int. J. Numer. Meth. Engng., Vol. 35, pp. 1351–1395, 1992.

[3] N. Vassart, R. Laporte and R. Motro, Determination of mechanism's order for kinematically and statically indeterminate systems, Int. J. Solids and Struct., Vol. 37 pp. 3807–3839, 2000.

[4] R. Liu, P. Serre and J. -F. Rameau, A tool to check mobility under parameter variation in over-constrained mechanisms, Mech. Machine Theory, Vol. 69, pp. 44–61, 2013.

[5] C. Chen, The order of local mobility mechanisms, Mech. Machine Theory, Vol. 46, pp. 1251–1264, 2011.

[6] M. Ohsaki and J. Y. Zhang, Stability conditions of prestresses pin-jointed structures, Int. J. Non-Linear Mech., Vol. 41, pp. 1109–1117, 2006.

[7] J. Y. Zhang and M. Ohsaki, Stability conditions for tensegrity structures, Int. J. Solids and Struct., Vol. 44(11-12), pp. 3875–3886, 2007.

[8] R. Connelly and W. Whiteley, Second-order rigidity and prestress stability for tensegrity frameworks, SIAM J. Discrete Math., Vol. 9(3), pp. 453–491, 1996.

[9] N. Katoh and S. Tanigawa, Rooted-tree decompositions with matroid constraints and the infinitesimal rigidity of frameworks with boundaries, SIAM J. Discrete Math., Vol. 27(1), pp. 155–185, 2013.

[10] W. T. Koiter, On the Stability of Elastic Equilibrium, Ph. D. Dissertation, Delft Univ. Tech., The Netherlands, 1945; English Translation, NASA, TTF-10833, 1967.

[11] J. Roorda and A. H. Chilver, Frame buckling: An illustration of the perturbation technique, Int. J. Non-Linear Mech., Vol. 5, pp. 235–246, 1970.

[12] J. M. T. Thompson and G. W. Hunt, A General Theory of Elastic Stability, John Wiley, New York, 2014.

[13] M. Ohsaki and K. Ikeda, Imperfection sensitivity of degenerate hilltop branching points, Int. J. Non-Linear Mech., Vol. 44, pp. 324–336, 2009.

[14] G. Garcea, G. Formica and R. Casciaro, A numerical analysis of infinitesimal mechanisms, Int. J. Numer. Meth. Engng., Vol. 62, pp. 979–1012, 2005.

[15] J. E. Baker, The Bennett, Goldberg and Myard linkages: In perspective, Mech. Machine Theory, Vol. 14, pp. 239–253, 1979.

[16] Y. Chen, Z. You and T. Tarnai, Threefold-symmetric Bricard linkages for deployable structures, Int. J. Solid Struct., Vol. 42, pp. 2287–2301, 2005.

[17] M. Ohsaki, Y. Kanno and S. Tsuda, Linear programming approach to design of spatial link mechanism with partially rigid joints, Struct. Multidisc. Optim., Vol. 50, pp. 945–956, 2014.

[18] M. Ohsaki and S. Tsuda and Y. Miyazu, Design of linkage mechanisms of partially rigid frames using limit analysis with quadratic yield functions Int. J. Solids and Struct., Vol. 88–89, pp. 68–78, 2016.

[19] J. C. Simo and L. Vu-Quoc, On the dynamics in space of rods undergoing large motions: A geometrically exact approach, Comp. Meth. Appl. Mech. Eng., Vol. 55, pp.125–161, 1988.

[20] K. M. Hsiao, J. Y. Lin and W. Y. Lin, A consistent co-rotational finite element formulation for geometrically nonlinear dynamic analysis of 3-D beams, Comp. Meth. Appl. Mech. Eng., Vol. 169, pp. 1–18, 1999.

[21] Z. X. Li, A co-rotational formulation for 3D beam element using vectorial rotational variables, Comp. Mech., Vol.39, pp. 309–322, 2007.

[22] S. D. Guest and P. W. Fowler, A symmetry-extended mobility rule, Int. J. Solids Struct., Vol. 40, pp. 1002–1004, 2005.

[23] H. Cheng and K. C. Gupta, An historical note on finite rotations, J. Appl. Mech., Vol. 56(1), pp. 139–145, 1989.

[24] E. J. Haug, Computer Aided Kinematics and Dynamics of Mechanical Systems: Vol. 1, Basic Methods, Allyn and Bacon, 1989,

[25] J. H. Ginsberg, Advanced Engineering Dynamics, Cambridge University Press, 1995.

[26] C. Meyer, Matrix Analysis and Applied Linear Algebra, SIAM, 2000.

[27] Maple User's Manual, Ver. 16, Maplesoft, 2016.

[28] Dassault Systm̀es, Abaqus User's Manual Ver. 6.14, 2014.